Published in final edited form as:
J Inherit Metab Dis. 2014 March ; 37(2): 297–308. doi:10.1007/s10545-013-9655-6.

Non-specific accumulation of glycosphingolipids in GNE myopathy

Katherine A. Patzel[1,2], **Tal Yardeni**[1,3], **Erell Le Poëc-Celic**[4], **Petcharat Leoyklang**[2], **Heidi Dorward**[2], **Dominic S. Alonzi**[1], **Nikolay V. Kukushkin**[1], **Bixue Xu**[5], **Yongmin Zhang**[5], **Matthieu Sollogoub**[5], **Yves Blériot**[5,6], **William A. Gahl**[2,7], **Marjan Huizing**[2,*], and **Terry D. Butters**[1,*]

[1] Oxford Glycobiology Institute, Department of Biochemistry, University of Oxford, Oxford, OX1 3QU, United Kingdom

[2] Medical Genetics Branch, National Human Genome Research Institute, National Institutes of Health, Bethesda MD, 20892, USA

[3] Graduate Partner Program, Sackler School of Medicine, Tel Aviv University, Tel Aviv, 69978, Israel

[4] Institut National Des Sciences Appliquées de Toulouse, Toulouse, 31400, France

[5] UPMC Université Paris 06, Institut Parisien de Chimie Monléculaire, Paris, 75005, France

[6] IC2MP, UMR, CNRS 7285, Université de Poitiers, Poitiers Cedex, 86022, France

[7] Office of Rare Diseases Research, Office of the Director, National Institutes of Health, Bethesda MD, 20892, USA

Abstract

Background—UDP-GlcNAc 2-epimerase/ManNAc 6-kinase (GNE) is a bifunctional enzyme responsible for the first committed steps in the synthesis of sialic acid, a common terminal monosaccharide in both protein and lipid glycosylation. GNE mutations are responsible for a rare autosomal recessive neuromuscular disorder, GNE myopathy (also called hereditary inclusion body myopathy). The connection between the impairment of sialic acid synthesis and muscle pathology in GNE myopathy remains poorly understood.

*To whom correspondence should be addressed. mhuizing@mail.nih.gov. Tel. (++1) 301 4022797. Fax (++1) 301 4807825. terry.butters@bioch.ox.ac.uk. Tel. (++44) 1865 275725. Fax. (44) (0) 1865 275216..

Author Contributions

Conception and design: KAP, TY, DSA, NVK, YB, MH, TDB Acquisition of data: KAP, TY, ELP-C, DSA, NVK, PL, HD, BX, MS Analysis and interpretation of data: KAP, TY, DSA, NVK, PL, HD, WAG, MH, TDB Drafting/revising and final approval of manuscript: KAP, TY, ELP-C, DSA, NVK, BX, YZ, MS, YB, WAG, MH, TDB
Final approval of manuscript: KAP, TY, ELP-C, DSA, NVK, PL, HD, BX, YZ, MS, YB, WAG, MH, TDB

Conflict of Interests

Katherine A. Patzel, Tal Yardeni, Erell Le Poëc-Celic, Dominic S. Alonzi, Nikolay V. Kukushkin, Bixue Xu, Yongmin Zhang, Matthieu Sollogoub, Yves Blériot, and Terry D. Butters declare that they have no conflict of interest.
Marjan Huizing and William A. Gahl are co-inventors on patent PCT/US2008/006895 “N- acetyl mannosamine as a therapeutic agent”.

Informed Consent

All procedures followed were in accordance with the ethical standards of the responsible committee on human experimentation (institutional and national) and with the Helsinki Declaration of 1975, as revised in 2000. Informed consent was obtained from all patients for being included in the study.

Animal Rights

All institutional and national guidelines for the care and use of laboratory animals were followed.

Methods—Glycosphingolipid (GSL) analysis was performed by HPLC in multiple models of GNE myopathy, including patients' fibroblasts and plasma, control fibroblasts with inhibited GNE epimerase activity through a novel imino sugar, and tissues of $Gne^{M712T/M712T}$ knock-in mice.

Results—Not only neutral GSLs, but also sialylated GSLs, were significantly increased compared to controls in all tested models of GNE myopathy. Treatment of GNE myopathy fibroblasts with N-acetylmannosamine (ManNAc), a sialic acid precursor downstream of GNE epimerase activity, ameliorated the increased total GSL concentrations.

Conclusion—GNE myopathy models have increased total GSL concentrations. ManNAc supplementation results in decrease of GSL levels, linking abnormal increase of total GSLs in GNE myopathy to defects in the sialic acid biosynthetic pathway. These data advocate for further exploring GSL concentrations as an informative biomarker, not only for GNE myopathy, but also for other disorders of sialic acid metabolism.

Introduction

GNE myopathy, also termed hereditary inclusion body myopathy (HIBM, IBM2; OMIM#600737) or distal myopathy with rimmed vacuoles (DMRV, Nonaka myopathy; OMIM#605820), is a rare autosomal recessive, neuromuscular disease. GNE myopathy is caused by *GNE* mutations, which encodes uridine diphosphate (UDP)-N-acetylglucosamine (GlcNAc) 2-epimerase/N-acetylmannosamine (ManNAc) 6-kinase (GNE), a key enzyme in sialic acid synthesis (**Supplementary Fig. S1**) (Eisenberg et al 2001; Hinderlich et al 1997; Keppler et al 1999). N-acetylneuraminic acid (Neu5Ac, commonly referred to as sialic acid) is the most common mammalian sialic acid, and the precursor of most other forms of sialic acids (Schauer 2009; Varki 1997; Varki 2008). Sialic acids are common terminal monosaccharides in both protein and lipid glycosylation where they provide a net negative charge and hydrophilicity that facilitate many functions, including roles in cell adhesion, signaling, and charge repulsion (Keppler et al 1999; Schauer 2009; Varki 1997; Varki 2008).

GNE myopathy patients' mutations (mostly missense) have been recorded throughout *GNE* and in a wide variety of ethnicities, with Japanese and Persian-Jewish genetic isolates (Eisenberg et al 2001; Eisenberg et al 2003; Huizing and Krasnewich 2009; Nishino et al 2002). Symptoms of GNE myopathy generally begin with distal muscle weakness in early adulthood. Muscle weakness both increases and spreads proximally, leaving patients wheelchair-bound approximately one to two decades post-onset (Argov and Yarom 1984; Nonaka et al 2005; Nonaka et al 1981). Biopsies of affected muscle characteristically display accumulations of autophagosomes often referred to as rimmed vacuoles (Malicdan et al 2007a; Malicdan et al 2007b; Nishino 2006; Nonaka et al 1998), cytoplasmic tubulofilamentous inclusions (Nonaka et al 1981), and intracellular deposition of β-amyloid and α-synuclein, as well as abnormally phosphorylated Tau (Askanas et al 1993; Askanas and Engel 1995).

A complete knock-out of the *Gne* gene in mice displayed early embryonic lethality (Schwarzkopf et al 2002). A *Gne* knock-in mouse model mimicking the p.M712T mutation, common among Persian-Jewish patients, unexpectedly died before 3 days of life (postnatal day 3, P3) of severe glomerular disease due to hyposialylation (Galeano et al 2007; Kakani et al 2012). Administration of the sialic acid precursor ManNAc increased survival of mutant $Gne^{M712T/M712T}$ pups beyond P3. Surviving mutants exhibited improved renal histology, increased levels of Gne protein and Gne-epimerase activities and increased glomerular sialylation (Galeano et al 2007; Kakani et al 2012). However, in GNE myopathy patients no indications of renal abnormalities have been reported. Humans and mice may differ in the relative importance of sialic acid to the kidney, and protein glycosylation patterns also vary (Chou et al 1998; Kershaw et al 1997). Mutant $Gne^{M712T/M712T}$ pups did

not live long enough to develop a muscle phenotype. However, in mutant pups rescued from neonatal lethality (by ManNAc administration or sporadic spontaneous survival) hyposialylation of muscle tissue can be detected by lectin staining at older ages (~4 months and older) (Niethamer et al 2012), similar to patients with GNE myopathy (Nemunaitis et al 2011; Nemunaitis et al 2010).

Despite the identification of impaired GNE activity in GNE myopathy, the connection between the impairment of sialic acid synthesis and muscle pathology remains poorly understood. Recent studies of the $Gne^{M712T/M712T}$ mouse model pointed to muscle-specific alterations in glycosphingolipid (GSL) levels (Paccalet et al 2010). We aimed to further investigate the global alterations in GSL levels in multiple models of GNE myopathy, including patients' fibroblasts and plasma samples, control fibroblasts with inhibited GNE epimerase activity, and tissues of the $Gne^{M712T/M712T}$ mouse model. Our studies provide compelling evidence that GSL concentrations can be an informative marker for GNE myopathy and likely other disorders with disruptions in the sialic acid synthesis pathway.

Materials and methods

Patients, primary fibroblasts and plasma

GNE myopathy patients were enrolled in a clinical protocol approved by the Institutional Review Board of the National Human Genome Research Institute (NHGRI) to investigate inborn errors of metabolism. Written informed consent was obtained from each patient. The diagnosis of GNE myopathy was based on clinical features, muscle pathology, and the presence of *GNE* gene mutations. Primary fibroblasts cultures were obtained from a skin biopsy. Plasma was obtained from two female patients, homozygous for the GNE p.M712T Persian-Jewish founder mutation, and three controls enrolled in clinical studies at the NIH.

Cell culture and compound treatments

Primary human fibroblasts were grown in DMEM (Invitrogen) supplemented with 10% Fetal Calf Serum (FCS, Invitrogen) containing 100 U/ml penicillin and 0.1 mg/ml streptomycin. HepG2 cells were grown in RPMI1640 medium (Invitrogen) containing 10% FCS, 2 mM L- glutamine, 100 U/ml penicillin, and 0.1 mg/ml streptomycin. For ManNAc supplementation, primary fibroblasts were grown to confluency in standard media containing 2% FCS with or without 10 mM ManNAc (Sigma). For GNE inhibitor treatments, fibroblasts were grown for one week in standard media containing 10% FCS, with or without acetamido trihydroxyazepane [22] (Li et al 2009) (α-D-*gluco*-like hexosaminidase inhibitor) in various concentrations. After a week, media were removed and replaced with media containing 2% FCS and same supplements as previously, followed by incubation for two weeks while cells reached confluency. Fibroblasts were harvested by scraping, pelleted by centrifugation and subjected to GSL extraction. Each data point represents an independent sample.

Animals

$Gne^{M712T/M712T}$ knock-in mice were generated using a murine targeting vector for homologous recombination in C57BL/6J embryonic stem cells constructed to include the p.M712T *Gne* mutation in exon 12 (ATG to ACG) (*Gne*, *Uae1*, GenBank NM_015828), as described (Galeano et al 2007). The mice were maintained in the C57BL/6J background. Animals were housed in an Association for Assessment and Accreditation of Laboratory Animal Care International–accredited specific pathogen–free facility in accordance with the *Guide for the care and use of laboratory animals* (NIH publication no. 85-23. Revised 1985). All mouse procedures were performed in accordance with protocol GO4-3 approved by the Institutional Animal Care and Use Committee or the National Human Genome

Research Institute. Mice were euthanized at P2. All experiments on mutant mouse tissues were performed on at least 5 wild type and 5 heterozygote mutant mice for each tissue (often littermates).

Glycosphingolipid analysis

Mouse tissues were dounce homogenised in the presence of protease inhibitor cocktail (Roche). Tissue extracts and fibroblasts were further lysed with three freeze-thaw cycles on dry ice in the presence of 0.1% Triton-X100. As described previously (Neville et al 2012), GSLs were extracted and purified, glycans released using Hirudo medicinalis ceramide glycanase (OGBI, Oxford, UK), labeled with anthranilic acid (2AA) and analysed by normal- phase high-performance liquid chromatography (HPLC).

GNE epimerase enzyme assay

The conversion of UDP-GlcNAc to ManNAc was assayed based on previously described methods (Sparks et al 2005). Confluent HepG2 cells were scraped and lysed in epimerase reaction buffer (0.2 M MES buffer, pH 7.2, containing 150 mM NaCl, 10 mM $CaCl_2$, 0.1 mM UDP, and 1% Triton-X100). Lysates were stored at −20°C until use in GNE epimerase reactions. HepG2 lysate in epimerase reaction buffer was added to UDP-GlcNAc (final concentration 100 μM) and $MgCl_2$ (final concentration 10 mM). Reactions were either immediately boiled for 1 min for baseline measurements, or incubated at 37°C for 1 hour (unless otherwise specified) before the reaction was stopped by boiling. Following the reaction, ManNAc was labeled with anthranilic acid (2-AA) (Sigma) and separated by Reverse-phase HPLC as described below. If used, acetamido trihydroxyazepane [22] imino sugar was added to GNE epimerase reactions with UDP-GlcNAc and $MgCl_2$.

Reverse-phase HPLC

Purified 2-AA-labeled monosaccharides were separated by reverse-phase HPLC using a 4.6×250 mm XTerra MS C_{18} 5um column (Waters) and Dionex DX 500 chromatography system with in-line Jasco FP-920 fluorescence detector. The gain was set to 1000 and the emission bandwidth to 40 nm. Chromatography was performed at 40°C. Solvent A was composed of 0.15% 1-butylamine, 0.5% H_2PO_4, and 1% THF in water. Solvent B was composed of 50% acetonitrile, 0.15% 1-butylamine, 0.5% H_2PO_4, and 1% THF in water. All chromatography was controlled, and data collected and processed using Dionex Chromeleon software for the DX 500 system, using the gradient: time = 0 (t=0), 95% A, 5% B (1 ml/min), t=7, 95% A, 5% B (1 ml/min), t=25, 82% A, 18% B (1 ml/min), t=27, 0% A, 100% B (1 ml/min), t=32, 0% A, 100% B (1 ml/min), t=34, 95% A, 5% B (1 ml/min), t=49 95% A, 5% B (1 ml/min). An aliquot (50 μl) of the 2-AA-labelled sample was added to 50 μl of acetonitrile. Samples containing 50 μl of acetonitrile, 45 μl of the labelled sample and 5 μl of ManNAc (Sigma), previously labelled with 2-AA were injected for identification of ManNAc retention time. Injection volume of 2-AA labelled material/acetonitrile was 50 μl.

Immunoblotting

Patients and control fibroblasts (cultured as described above) pellets were lysed in 50 mM Tris, 300 mM NaCl, 0.5% Triton, and 5 mM EDTA in the presence of protease inhibitors (Complete Mini; Roche Applied Science, Mannheim, Germany). Selected control samples were desialylated by incubation with 1 μl (50U) neuraminidase (NA) for 1 hour at a 37^0C (P0728, New England Biolabs, Ipswich, MA). Total protein concentrations were measured by the DC Protein assay (Bio-Rad Laboratories, Hercules, CA). Total protein extracts (20 μg) were mixed with 5X sample loading buffer for SDS PAGE (GenScript, Piscataway, NJ), boiled at 95^0 C for 5 min, and loaded onto 4-12% Tris-Glycine gels (Invitrogen), followed by electroblotting onto nitrocellulose membranes (Invitrogen). The membranes were probed

with mouse monoclonal anti-LAMP1 (H4A3-S) or anti-LAMP-2 (H4B4-S) antibodies (both from Developmental Studies Hybridoma Bank, University of Iowa, IO) or rabbit polyclonal anti-CD63 antibodies (H-193; Santa Cruz Biotechnology, Santa Cruz, CA). Anti β-actin (Clone AC-15) or anti-α-tubulin (Clone B-5-1-2) antibody (both from Sigma Aldrich, St. Louis, MO) labeling was used as loading control. Detection was performed with anti-mouse or anti-rabbit secondary IRDye800CW-conjugated antibodies for Li-Cor Odyssey Infrared detection (Li-Cor Biosciences, Lincoln, NE).

Immunofluorescence

Patients and control fibroblasts (cultured as described above) were seeded onto Lab-Tek Chamber Slides (Nunc, Thermoscientific Roskilde, Denmark) and grown overnight. For antibody staining, the cells were fixed with 3% paraformaldehyde, blocked in phosphate buffered saline (PBS), 2% donkey serum, 1% saponin, and 5% glycine. Cells were then incubated overnight with mouse monoclonal anti-LAMP-2 or anti-CD63 antibodies (H4B4 or H5C6; Developmental Studies Hybridoma Bank, University of Iowa) in PBS, 2% bovine serum albumin (BSA), 1% saponin, followed by secondary anti-mouse Alexa Fluor 555 (Invitrogen). For endocytosis studies, cells were inclubated 45 min in culture medium containing 1 mg/ml Dextran Alexafluor 488 (10,000 MW-fixable, D22910; Invitrogen), followed by washout with PBS and fixation in 3% paraformaldehyde. All fluorescent labeled cells were mounted with Vectasheld (Vector Laboratories, Burlingame, CA). All imaging was performed on a Zeiss LSM 510META confocal laser-scanning Microscopy (Carl Zeiss, Jena, Germany). All presented images are 1D projections of confocal Z-stacks.

Statistical analysis

Conventional statistical methods were employed to calculate mean values and standard errors of the mean (SEM). Differences between groups were tested for significance using two-tailed Student’s t-test for unpaired observations.

Results

GSL levels are increased in primary GNE myopathy fibroblasts

To measure GSL concentrations in primary fibroblast cell lines isolated from skin biopsies of patients with *GNE* myopathy, we used HPLC analysis of fluorescently labeled glycans released from lipids (**Fig. 1A**). Patients’ fibroblasts carrying missense mutations throughout *GNE* (**Fig. 1B**) were used, allowing for the study of mutations in either or both the epimerase and the kinase domains of GNE. These cell lines will further be referred to as patient 1 (carrying two epimerase domain mutations, p.R335W/L347del;H348N), patient 2 (carrying one epimerase domain mutations, p.V216A, and one kinase domain mutation, p.A631V), patient 3 (homozygous for the Persian-Jewish founder kinase domain mutation, p.M712T), and patient 4 (carrying two epimerase domain mutations, p.G135V/R246W).

Eight GSL-derived oligosaccharide species were identified in human fibroblasts, with Gb3 being the major peak (**Fig. 1C**). Although the changes in individual GSL species varied depending on the *GNE* mutations, all patient derived cell lines displayed a trend of significantly increased total GSL concentration (**Fig. 1D**). Surprisingly, concentrations of both neutral and sialylated GSL species were significantly increased in patient-derived cell lines when compared to control fibroblast (**Fig. 1E**). Compared to controls, fibroblasts from patient 1 demonstrated significantly higher concentrations of neutral Gb3, Gb4, and PG. Patient 2 fibroblasts showed significantly increased expression of Gb3, Gb4, and, unexpectedly, sialylated GM3, GM2, and GM1a. Similarly, patient 3 fibroblasts had significantly increased neutral Gb3, Gb4, PG, and sialylated GM3 and GM2.

The changes in GSL concentrations in GNE myopathy fibroblasts could not be explained by increases in a single GSL biosynthesis series. All patients' fibroblasts showed a significant increase in the neutral *globo*-series (**Fig. 1F**). The *a*-series, containing sialylated GSL species, was also increased in all patients' cell lines (significant in patient 2 and patient 3, carrying a kinase domain mutation). For the weakly expressed *neolacto*-series GSLs, patients 1 and 3 displayed increased concentrations compared to controls. Only *b*-series GSLs, consisting in fibroblast cells solely of minimally expressed GD3, had decreased expression in patients' cell lines (significant only for patient 3).

Increase in GSL levels results from decreased sialic acid synthesis due to impaired GNE function

The mechanisms by which mutated GNE can increase levels of both sialylated and neutral GSLs remain unclear. The nuclear localization of GNE (Krause et al 2005), the binding of GNE to proteins such as CRMP-1, PLZF (Weidemann et al 2006), and α-actinin (Amsili et al 2008), the existence of multiple alternatively spliced GNE transcripts (Yardeni et al 2011), and the oligomer formation of GNE (Ghaderi et al 2007) have led to speculation that GNE may have additional functions outside of sialic acid synthesis (Wang et al 2006). To test whether increased GSL concentrations are directly linked to the impairment of sialic acid synthesis or, alternatively, to a yet undefined function of GNE, fibroblasts were grown in media supplemented with ManNAc or the GNE epimerase activity inhibitor acetamido trihydroxyazepane.

ManNAc supplementation was previously shown to increase sialic acid concentrations and glycoprotein sialylation (Galeano et al 2007; Jones et al 2004; Kakani et al 2012; Keppler et al 1999; Malicdan et al 2009; Malicdan et al 2012; Noguchi et al 2004; Schwarzkopf et al 2002). Notably, ManNAc supplementation can increase sialylation despite GNE kinase domain mutations (as seen in some GNE myopathy patients) due to ManNAc phosphorylation by promiscuous kinases, in particular GlcNAc kinase (Hinderlich et al 2001). Since cells in culture can recycle monosaccharides from glycans found in FCS (Schwarzkopf et al 2002) decreasing the requirement for *de novo* synthesis of sialic acid, control and GNE myopathy patients' fibroblasts were grown in serum-deprived conditions (2% FCS) with or without 10 mM ManNAc. All cell lines including controls exhibited increased GSL concentrations in serum deprived conditions when compared to standard 10% FCS conditions (data not shown). Changes in control lines with reduced FCS may be explained by low GNE expression in this cell line. It is likely that even in control conditions some amount of glycan recycling is required to maintain standard sialic acid levels. Both GNE myopathy and control fibroblasts showed a significant decrease in total GSLs when grown in the presence of ManNAc (**Fig. 2A, B**). Importantly, a significant reduction was observed in Gb3, GM3, and Gb4 (**Supplementary Fig. S2**), GSL species that were significantly increased in untreated GNE myopathy cell lines compared to control (**Fig. 1E**).

These data imply that the connection between impaired GNE function and increased levels of GSLs stems from the role of the enzyme in the biosynthesis of sialic acid. We implicate reduced bioavailability of sialic acid in the abnormal accumulation of cellular GSLs.

Polyhydroxylated azacycles, or imino sugars, are potent inhibitors of glycosidases. Imino sugars act as monosaccharide mimics due to their ability to adopt similar spatial conformations to monosaccharides (Alonzi and Butters 2011; Butters et al 2000). A series of imino sugars mimicking the charged transition state of GlcNAc were reported to have inhibitory activity against GNE epimerase (Al-Rawi et al 2004). Here, we tested an acetamido trihydroxyazepane imino sugar (acetamido trihydroxyazepane [22]; **Fig. 2C**), a D- gluco-like hexosaminidase inhibitor (Li et al 2009) for inhibitory activity against GNE epimerase enzymatic activity. We developed a GNE epimerase enzymatic assay based on

the work of Sparks et al. (Sparks et al 2005). Epimerase activity was measured through the production of ManNAc in HepG2 cell lysates after addition of UDP-GlcNAc. The human liver carcinoma cell line, HepG2, was chosen for these experiments due to high expression of the *GNE* gene in human liver (Lucka et al 1999). Analysis over a range of concentrations revealed potent inhibition with an IC_{50} around 10 μM (**Supplementary Fig. S3**). GNE myopathy fibroblasts grown in the presence of the acetamido trihydroxyazepane displayed a dose-dependent increase in already elevated GSL concentrations, regardless of the cell line genotype (**Fig. 2D, E**). In control fibroblasts, acetamido trihydroxyazepane addition also induced a GNE myopathy-like increase in GSL levels, although, as expected, the concentration of the compound required to induce a significant effect was higher than that for GNE myopathy cell lines (**Fig. 2E**). Both neutral and sialylated GSL species showed a trend towards increase in all cell lines following treatment with 100 μ M acetamido trihydroxyazepane (**Supplementary Fig. S4**) as were absolute amounts of GSLs in all series (results not shown). These experiments add further evidence to support a negative correlation between sialic acid biosynthetic capability and total GSL concentrations.

GSL concentrations are increased in GNE myopathy patient plasma

Plasma from three control and two female patients with GNE myopathy homozygous for the p.M712T founder mutation were analysed for GSL concentrations. Twelve GSL-derived oligosaccharides were detected, ten of which could be identified by comparison of glucose unit values to a standard GSL-derived glycan database (**Fig. 3A,C**). Although the limited sample set did not allow statistical analysis, an increase in total GSL was observed in both patients' plasma samples (mean 0.0055 pmol/μg of protein in GNE myopathy patients *vs* mean 0.0029 pmol/μg of protein in controls) (**Fig. 3B**). Similar trends were observed for several individual GSL species (**Fig. 3C**). Although preliminary, our evidence presents an intriguing possibility that increased plasma levels of GSLs could be employed as a potential marker of GNE myopathy. Further investigation to include increased sample sizes, as well as patients with mutations throughout GNE is essential.

GSL levels are increased in $Gne^{M712T/M712T}$ mice

To evaluate the *in vivo* relevance of our findings of increased GSL levels in GNE myopathy patients' plasma and fibroblasts, we employed the $Gne^{M712T/M712T}$ knock-in mouse model. As described, mutant $Gne^{M712T/M712T}$ mice die before P3 of severe glomerular disease due to hyposialylation (Galeano et al 2007). Due to lack of a better animal model (such as a muscle- specific knock-in model), GSL analysis was performed on $Gne^{M712T/M712T}$ knock-in mice sacrificed at P2. Although there were no significant changes at this age in total GSL concentrations in the five tissues tested, including gluteus (skeletal muscle), kidney, heart, liver and brain (**Fig 4A**), significant changes in individual GSL species were detected.

Skeletal muscle, the only affected tissue in GNE myopathy patients, demonstrated significantly increased levels of several GSL species including neutral Gb3, Gb4, and PG, as well as sialylated 2,3-SPG (**Fig. 4B**). Previously reported decreases in GM3 in 4 to 6 month old mutant mice (Paccalet et al 2010) were not observed at P2. Our preliminary data suggest that this discrepancy is unlikely to be due to age, but may be explained by the muscle tested, gluteus rather than gastrocnemius (Paccalet et al 2010), or normalization, protein concentration rather than wet weight (Paccalet et al 2010).

In agreement with previous studies (Paccalet et al 2010), no significant differences in GSL concentrations were observed in kidney, heart, and liver. In mutant brain, an unidentified GSL species was significantly increased when compared to age-matched controls. These data suggest that skeletal muscle, the only tissue affected in GNE myopathy patients, is

particularly susceptible to increases in GSL concentrations, which likely result from impairment of sialic acid biosynthesis.

Endo-lysosomal markers in GNE myopathy fibroblasts

Selected endosomal markers were used to evaluate the endocytic vesicular system in GNE myopathy fibroblasts that could help explain the global increase of GSL species. Distribution of the fluid-phase endocytosis marker dextran appeared similar in GNE myopathy fibroblasts compared to control cells (**Supplementary Fig. S5A)**. Likewise, immunofluorescence studies showed a normal cellular distribution of the endo-lysosomal membrane markers LAMP-2 and CD63 (**Supplementary Fig. S5B)**. Immunoblotting assays with the membrane markers LAMP-1, LAMP-2 and CD63 showed a decreased expression of all three markers in GNE myopathy fibroblasts compared to control fibroblasts. In addition, LAMP-1 and LAMP- 2 proteins exhibited a slightly decreased molecular weight (illustrated by a downshift on the immunoblot), similar to neuraminidase-treated control fibroblast extracts (**Supplementary Fig. S5C)**.

Discussion

In the present study, we sought to investigate GSL levels in models of GNE myopathy. Our global GSL analysis found consistent and significant increases in both sialylated and neutral species in multiple models of GNE myopathy. First, cultured fibroblasts isolated from GNE myopathy patients showed unspecific increases in GSL concentrations, which decreased following ManNAc supplementation to bypass the requirement for GNE enzymatic activity in the sialic acid biosynthesis pathway. Second, GSL expression in control fibroblasts was increased following pharmacological inhibition of GNE epimerase activity using a novel imino-sugar inhibitor. Third, plasma samples of GNE myopathy patients showed increased GSLs. And finally, skeletal muscle of a GNE myopathy knock-in mouse model showed a trend towards increased GSL levels at postnatal day 2.

Our results provide evidence that impaired biosynthesis of sialic acid causes an accumulation of GSLs in mammalian cells. Surprisingly, this not only affects neutral, but to the same extent charged, sialylated, GSLs, which appears counterintuitive since enhanced sialylation in the conditions of sialic acid deprivation appears unlikely. If biosynthesis of GSLs was increased globally in sialic acid-deficient cells, elevation of neutral-to-charged GSL ratio would be expected, which is not supported by our data. Additionally, we did not succeed in detecting an increase in GM3 synthase, one of the major enzymes in GSL biosynthesis, in P2 mice or older animals rescued by ManNAc treatment (data not shown). Overall, the observed accumulation of GSLs following impairment of GNE function is unlikely to be mediated via enhanced glycolipid biosynthesis. We therefore propose that the effect is a consequence of impairment of GSL degradation.

GSL catabolism begins when fragments of plasma membrane containing GSLs targeted for degradation are endocytosed in coated pits and trafficked through the endosomal pathway to the lysosome as intralysosomal structures (Huwiler et al 2000). Unlike in inherited glycosphingolipid storage diseases when a deficiency in a particular catabolic enzyme causes an accumulation of individual GSL species, the build-up of GSLs observed in GNE myopathy is not specific. Such a global increase in all detectable GSL species likely indicates a lesion earlier in the endocytosis-endosome-lysosome pathway.

Distribution of the endocytic fluid phase marker dextran appeared normal in GNE myopathy fibroblasts, suggesting a normal endocytic pathway (**Supplementary Fig. 5A**). However, while the glycosylated endo-lysosomal membrane markers LAMP-1, LAMP-2 and CD63 showed a normal intracellular distribution (**Supplementary Fig. 5B**), their expression was

decreased in GNE myopathy fibroblasts (**Supplementary Fig 5C**). In addition, LAMP-1 and LAMP-2 appeared to be aberrantly glycosylated.

Interestingly, a group of myopathies such as Pompe disease, Danon disease (LAMP-2 deficiency) and X-linked myopathy with excessive autophagy (XMEA), characterised by a progressive course of muscle weakness and accumulation of autophagic vacuoles - symptoms typical of GNE myopathy - display impairment of lysosomal function (Malicdan and Nishino 2012; Malicdan et al 2008; Nishino 2006; Ramachandran et al 2009).

We propose a model for GNE myopathy in which a decrease in the rate of sialic acid biosynthesis causes disruption of the endocytosis-endosome-lysosome pathway, possibly through hyposialylation of essential glycoprotein(s) mediating one of the steps in the process. Attractive candidates for such are LAMP-1 and LAMP-2, a highly glycosylated lysosomal proteins, deficiencies of which may cause impairment of lysosomal pathways (Eskelinen 2006), which may in turn lead to progressive accumulation of GSLs. These findings warrant future research, beyond the scope of this paper, with a wider variety of membrane and fluid- phase endosomal markers to further investigate whether defects in the complex endo- lysosomal system underlie the increase in GSL species.

Our proposed model can also account for apparent contradictions between our data and that in the published literature. Wang et al previously reported decreased levels of GM3 and GD3 with siRNA and shRNA knockdown of *GNE* in HEK AD293 cells (Wang et al 2006). However GM3 and GD3 levels were measured using FACs, a technique which measures GSLs on the plasma membrane while our HPLC method measures GSLs throughout the cell. If a decrease in sialic acid biosynthesis interrupts the endocytosis- endosome-lysosome pathway we would expect GSLs to be aberrantly stored on vesicles within the cell rather than the cell surface leading to very different interpretations using these different techniques.

GNE myopathy fibroblasts have elevated GSL expression in normal growth conditions, implying that they cannot synthesise or incorporate extracellular sources of sialic acid efficiently. When GNE myopathy cells are grown in serum-deprived conditions, GSL levels further increase. These findings predict that in conditions of sialic acid deprivation, recycling of extracellular nutrients would also be impaired. This impairment may over time affect sialylation and function of crucial membrane glycans of the endosomal-lysosomal pathway, further limiting the access to extracellular sialic acid. This model may also offer insight into the late onset and progressive nature of myopathic symptoms of GNE myopathy.

In summary, GSL concentrations have been shown to be sensitive to lesions in the sialic acid synthesis pathway. Here we demonstrate non-specific accumulation of GSLs in GNE myopathy, which might serve as a useful marker of the disease, in addition to previously suggested sialylation status of neural cell adhesion molecule (NCAM) (Valles-Ayoub et al 2012). GSLs may also be explored as markers of other diseases with aberrant sialic acid metabolism since they can be non-invasively measured in unaffected tissues such as blood.

Supplementary Material

Refer to Web version on PubMed Central for supplementary material.

Acknowledgments

The authors thank Professor Raymond Dwek for his support (Oxford Glycobioloby Institute). We thank Shelley Hoogstraten-Miller and Theresa Calhoun (NHGRI, NIH) for their skilled assistance with mouse maintenance and thank Carla Ciccone and Heidi Dorward (NHGRI, NIH) for their her expert laboratory work. We thank the HIBM Research Group (Encino, CA, USA) for providing the *Gne* M712T knock-in mouse model.

Funding

This work was supported by the Oxford Glycobiology Institute, Oxford, UK (K.A.P., D.S.A., N.V.K., and T.D.B.), l'Association "Vaincre les maladies lysosomales" (Y.B.) and the Intramural Research Programs of the National Human Genome Research Institute, National Institutes of Health, Bethesda, MD, USA (K.A.P., T.Y., P.L., H.D., W.A.G., and M.H.). The authors confirm independence from the sponsors; the content of the article has not been influenced by the sponsors.

Abbreviations

2-AA	anthranilic acid
CMP	cytidine monophosphate
CMP-SA	CMP-sialic acid
CTP	cytidine triphosphate
DMRV	distal myopathy with rimmed vacuoles
ECL	enhanced chemiluminescence
FCS	fetal calf serum
GlcNAc	N-acetyl glucosamine
GNE	UDP-GlcNAc 2-epimerase/ManNAc 6-kinase
GSL	glycosphingolipid
HIBM	hereditary inclusion body myopathy
HPLC	high-performance liquid chromatography
HRP	horseradish peroxidase
ManNAc	N-acetylmannosamine
MES	2-(N-morpholino)ethanesulfonic acid
Neu5AC	N-acetylneuraminic acid or sialic acid
NP-HPLC	normal-phase HPLC
OMIM	Online Mendelian Inheritance in Man
PVDF	polyvinylidene fluoride
RP-HPLC	reverse-phase HPLC
SDS-PAGE	sodium dodecyl sulfate polyacrylamide gel electrophoresis
SEM	standard error of the mean
THF	tetrahydrofuran
UDP	uridine diphosphate
XMEA	X-linked myopathy with excessive autophagy

References

Al-Rawi S, Hinderlich S, Reutter W, Giannis A. Synthesis and biochemical properties of reversible inhibitors of UDP-N-acetylglucosamine 2-epimerase. Angew Chem Int Ed Engl. 2004; 43:4366–4370. [PubMed: 15368395]

Alonzi DS, Butters TD. Therapeutic targets for inhibitors of glycosylation. Chimia (Aarau). 2011; 65:35–39. [PubMed: 21469442]

Amsili S, Zer H, Hinderlich S, et al. UDP-N-acetylglucosamine 2-epimerase/N-acetylmannosamine kinase (GNE) binds to alpha-actinin 1: novel pathways in skeletal muscle? PLoS One. 2008; 3:e2477. [PubMed: 18560563]

Argov Z, Yarom R. “Rimmed vacuole myopathy” sparing the quadriceps. A unique disorder in Iranian Jews. J Neurol Sci. 1984; 64:33–43.

Askanas V, Alvarez RB, Engel WK. beta-Amyloid precursor epitopes in muscle fibers of inclusion body myositis. Ann Neurol. 1993; 34:551–560. [PubMed: 7692809]

Askanas V, Engel WK. New advances in the understanding of sporadic inclusion-body myositis and hereditary inclusion-body myopathies. Curr Opin Rheumatol. 1995; 7:486–496. [PubMed: 8579968]

Butters TD, Dwek RA, Platt FM. Inhibition of glycosphingolipid biosynthesis: application to lysosomal storage disorders. Chem Rev. 2000; 100:4683–4696. [PubMed: 11749362]

Chou HH, Takematsu H, Diaz S, et al. A mutation in human CMP-sialic acid hydroxylase occurred after the Homo-Pan divergence. Proc Natl Acad Sci U S A. 1998; 95:11751–11756. [PubMed: 9751737]

Eisenberg I, Avidan N, Potikha T, et al. The UDP-N-acetylglucosamine 2-epimerase/N-acetylmannosamine kinase gene is mutated in recessive hereditary inclusion body myopathy. Nat Genet. 2001; 29:83–87. [PubMed: 11528398]

Eisenberg I, Grabov-Nardini G, Hochner H, et al. Mutations spectrum of GNE in hereditary inclusion body myopathy sparing the quadriceps. Hum Mutat. 2003; 21:99. [PubMed: 12497639]

Eskelinen EL. Roles of LAMP-1 and LAMP-2 in lysosome biogenesis and autophagy. Mol Aspects Med. 2006; 27:495–502. [PubMed: 16973206]

Galeano B, Klootwijk R, Manoli I, et al. Mutation in the key enzyme of sialic acid biosynthesis causes severe glomerular proteinuria and is rescued by N-acetylmannosamine. J Clin Invest. 2007; 117:1585–1594. [PubMed: 17549255]

Ghaderi D, Strauss HM, Reinke S, et al. Evidence for dynamic interplay of different oligomeric states of UDP-N-acetylglucosamine 2-epimerase/N-acetylmannosamine kinase by biophysical methods. J Mol Biol. 2007; 369:746–758. [PubMed: 17448495]

Hinderlich S, Berger M, Keppler OT, Pawlita M, Reutter W. Biosynthesis of N-acetylneuraminic acid in cells lacking UDP-N-acetylglucosamine 2-epimerase/N-acetylmannosamine kinase. Biol Chem. 2001; 382:291–297. [PubMed: 11308027]

Hinderlich S, Stasche R, Zeitler R, Reutter W. A bifunctional enzyme catalyzes the first two steps in N-acetylneuraminic acid biosynthesis of rat liver. Purification and characterization of UDP-N-acetylglucosamine 2-epimerase/N-acetylmannosamine kinase. J Biol Chem. 1997; 272:24313–24318. [PubMed: 9305887]

Huizing M, Krasnewich DM. Hereditary inclusion body myopathy: a decade of progress. Biochim Biophys Acta. 2009; 1792:881–887. [PubMed: 19596068]

Huwiler A, Kolter T, Pfeilschifter J, Sandhoff K. Physiology and pathophysiology of sphingolipid metabolism and signaling. Biochim Biophys Acta. 2000; 1485:63–99. [PubMed: 10832090]

Jones MB, Teng H, Rhee JK, et al. Characterization of the cellular uptake and metabolic conversion of acetylated N-acetylmannosamine (ManNAc) analogues to sialic acids. Biotechnol Bioeng. 2004; 85:394–405. [PubMed: 14755557]

Kakani S, Yardeni T, Poling J, et al. The Gne M712T mouse as a model for human glomerulopathy. Am J Pathol. 2012; 180:1431–1440. [PubMed: 22322304]

Keppler OT, Hinderlich S, Langner J, et al. UDP-GlcNAc 2-epimerase: a regulator of cell surface sialylation. Science. 1999; 284:1372–1376. [PubMed: 10334995]

Kershaw DB, Beck SG, Wharram BL, et al. Molecular cloning and characterization of human podocalyxin-like protein. Orthologous relationship to rabbit PCLP1 and rat podocalyxin. J Biol Chem. 1997; 272:15708–15714. [PubMed: 9188463]

Krause S, Hinderlich S, Amsili S, et al. Localization of UDP-GlcNAc 2-epimerase/ManAc kinase (GNE) in the Golgi complex and the nucleus of mammalian cells. Exp Cell Res. 2005; 304:365–379. [PubMed: 15748884]

Li H, Marcelo F, Bello C, et al. Design and synthesis of acetamido tri- and tetra- hydroxyazepanes: potent and selective beta-N-acetylhexosaminidase inhibitors. Bioorg Med Chem. 2009; 17:5598–5604. [PubMed: 19592259]

Lucka L, Krause M, Danker K, Reutter W, Horstkorte R. Primary structure and expression analysis of human UDP-N-acetyl-glucosamine-2-epimerase/N-acetylmannosamine kinase, the bifunctional enzyme in neuraminic acid biosynthesis. FEBS Lett. 1999; 454:341–344. [PubMed: 10431835]

Malicdan MC, Nishino I. Autophagy in lysosomal myopathies. Brain Pathol. 2012; 22:82–88. [PubMed: 22150923]

Malicdan MC, Noguchi S, Hayashi YK, Nonaka I, Nishino I. Prophylactic treatment with sialic acid metabolites precludes the development of the myopathic phenotype in the DMRV-hIBM mouse model. Nat Med. 2009; 15:690–695. [PubMed: 19448634]

Malicdan MC, Noguchi S, Nishino I. Autophagy in a mouse model of distal myopathy with rimmed vacuoles or hereditary inclusion body myopathy. Autophagy. 2007a; 3:396–398. [PubMed: 17471014]

Malicdan MC, Noguchi S, Nonaka I, Hayashi YK, Nishino I. A Gne knockout mouse expressing human GNE D176V mutation develops features similar to distal myopathy with rimmed vacuoles or hereditary inclusion body myopathy. Hum Mol Genet. 2007b; 16:2669–2682. [PubMed: 17704511]

Malicdan MC, Noguchi S, Nonaka I, Saftig P, Nishino I. Lysosomal myopathies: an excessive build-up in autophagosomes is too much to handle. Neuromuscul Disord. 2008; 18:521–529. [PubMed: 18502640]

Malicdan MC, Noguchi S, Tokutomi T, et al. Peracetylated N-acetylmannosamine, a synthetic sugar molecule, efficiently rescues muscle phenotype and biochemical defects in mouse model of sialic acid-deficient myopathy. J Biol Chem. 2012; 287:2689–2705. [PubMed: 22157763]

Nemunaitis G, Jay CM, Maples PB, et al. Hereditary Inclusion Body Myopathy: Single Patient Response to Intravenous Dosing of GNE Gene Lipoplex. Hum Gene Ther. 2011; 22:1331–1341. [PubMed: 21517694]

Nemunaitis G, Maples PB, Jay C, et al. Hereditary inclusion body myopathy: single patient response to GNE gene Lipoplex therapy. J Gene Med. 2010; 12:403–412. [PubMed: 20440751]

Neville DC, Alonzi DS, Butters TD. Hydrophilic interaction liquid chromatography of anthranilic acid-labelled oligosaccharides with a 4-aminobenzoic acid ethyl ester-labelled dextran hydrolysate internal standard. J Chromatogr A. 2012; 1233:66–70. [PubMed: 22391491]

Niethamer TK, Yardeni T, Leoyklang P, et al. Oral monosaccharide therapies to reverse renal and muscle hyposialylation in a mouse model of GNE myopathy. Mol Genet Metab. 2012; 107:748–755. [PubMed: 23122659]

Nishino I. Autophagic vacuolar myopathy. Semin Pediatr Neurol. 2006; 13:90–95. [PubMed: 17027858]

Nishino I, Noguchi S, Murayama K, et al. Distal myopathy with rimmed vacuoles is allelic to hereditary inclusion body myopathy. Neurology. 2002; 59:1689–1693. [PubMed: 12473753]

Noguchi S, Keira Y, Murayama K, et al. Reduction of UDP-N-acetylglucosamine 2-epimerase/N-acetylmannosamine kinase activity and sialylation in distal myopathy with rimmed vacuoles. J Biol Chem. 2004; 279:11402–11407. [PubMed: 14707127]

Nonaka I, Murakami N, Suzuki Y, Kawai M. Distal myopathy with rimmed vacuoles. Neuromuscul Disord. 1998; 8:333–337. [PubMed: 9673988]

Nonaka I, Noguchi S, Nishino I. Distal myopathy with rimmed vacuoles and hereditary inclusion body myopathy. Curr Neurol Neurosci Rep. 2005; 5:61–65. [PubMed: 15676110]

Nonaka I, Sunohara N, Ishiura S, Satoyoshi E. Familial distal myopathy with rimmed vacuole and lamellar (myeloid) body formation. J Neurol Sci. 1981; 51:141–155. [PubMed: 7252518]

Paccalet T, Coulombe Z, Tremblay JP. Ganglioside GM3 levels are altered in a mouse model of HIBM: GM3 as a cellular marker of the disease. PLoS One. 2010; 5:e10055. [PubMed: 20383336]

Ramachandran N, Munteanu I, Wang P, et al. VMA21 deficiency causes an autophagic myopathy by compromising V-ATPase activity and lysosomal acidification. Cell. 2009; 137:235–246. [PubMed: 19379691]

Schauer R. Sialic acids as regulators of molecular and cellular interactions. Curr Opin Struct Biol. 2009; 19:507–514. [PubMed: 19699080]

Schwarzkopf M, Knobeloch KP, Rohde E, et al. Sialylation is essential for early development in mice. Proc Natl Acad Sci U S A. 2002; 99:5267–5270. [PubMed: 11929971]

Sparks SE, Ciccone C, Lalor M, et al. Use of a cell-free system to determine UDP-N-acetylglucosamine 2-epimerase and N-acetylmannosamine kinase activities in human hereditary inclusion body myopathy. Glycobiology. 2005; 15:1102–1110. [PubMed: 15987957]

Valles-Ayoub Y, Esfandiarifard S, Sinai P, et al. Serum neural cell adhesion molecule is hyposialylated in hereditary inclusion body myopathy. Genet Test Mol Biomarkers. 2012; 16:313–317. [PubMed: 22085395]

Varki A. Sialic acids as ligands in recognition phenomena. FASEB J. 1997; 11:248–255. [PubMed: 9068613]

Varki A. Sialic acids in human health and disease. Trends Mol Med. 2008; 14:351–360. [PubMed: 18606570]

Wang Z, Sun Z, Li AV, Yarema KJ. Roles for UDP-GlcNAc 2-epimerase/ManNAc 6-kinase outside of sialic acid biosynthesis: modulation of sialyltransferase and BiP expression, GM3 and GD3 biosynthesis, proliferation, and apoptosis, and ERK1/2 phosphorylation. J Biol Chem. 2006; 281:27016–27028. [PubMed: 16847058]

Weidemann W, Stelzl U, Lisewski U, et al. The collapsin response mediator protein 1 (CRMP-1) and the promyelocytic leukemia zinc finger protein (PLZF) bind to UDP-N-acetylglucosamine 2-epimerase/N-acetylmannosamine kinase (GNE), the key enzyme of sialic acid biosynthesis. FEBS Lett. 2006; 580:6649–6654. [PubMed: 17118363]

Wennekes T, van den Berg RJ, Boot RG, et al. Glycosphingolipids--nature, function, and pharmacological modulation. Angew Chem Int Ed Engl. 2009; 48:8848–8869. [PubMed: 19862781]

Yardeni T, Choekyi T, Jacobs K, et al. Identification, tissue distribution, and molecular modeling of novel human isoforms of the key enzyme in sialic acid synthesis, UDP- GlcNAc 2-epimerase/ManNAc kinase. Biochemistry. 2011; 50:8914–8925. [PubMed: 21910480]

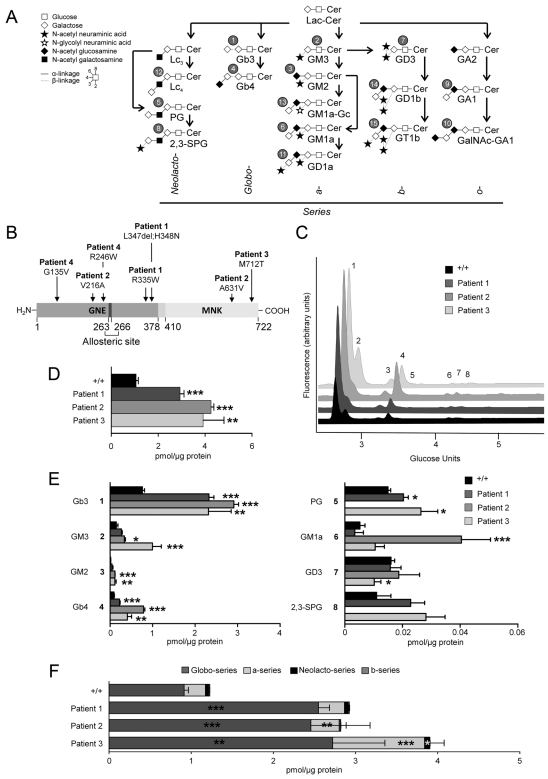

Fig. 1. GSL concentrations are increased in GNE myopathy patients' fibroblasts

A: The GSL biosynthesis pathway. GSL glycan structures follow the Oxford standard system for carbohydrate diagrams. For further details on GSL biosynthesis please see Wennekes et al (Wennekes et al 2009).

B: Schematic structure of the GNE protein with mutations in GNE myopathy patients' fibroblasts, epimerase enzymatic domain (GNE), kinase enzymatic domain (MNK), and allosteric site are indicated.

C: HPLC analysis of 2-AA labeled GSL-derived oligosaccharides isolated from control (+/+) and GNE myopathy patients' fibroblasts grown in 10% FCS. Peak numbers refer to GSL species in Figure 1A.

D: Total GSL measurements from control (+/+) and GNE myopathy patients' fibroblasts grown in 10% FCS.

E: Comparison of individual GSL concentrations in control (+/+) and GNE myopathy patients' fibroblasts grown in 10% FCS.

F: GSL concentrations analysed by series in control (+/+) and GNE myopathy patients' fibroblasts. Bars represent mean ± SEM (n=3) *P<0.05, **P<0.01, ***P<0.001 (two-tailed unpaired Student's t-test).

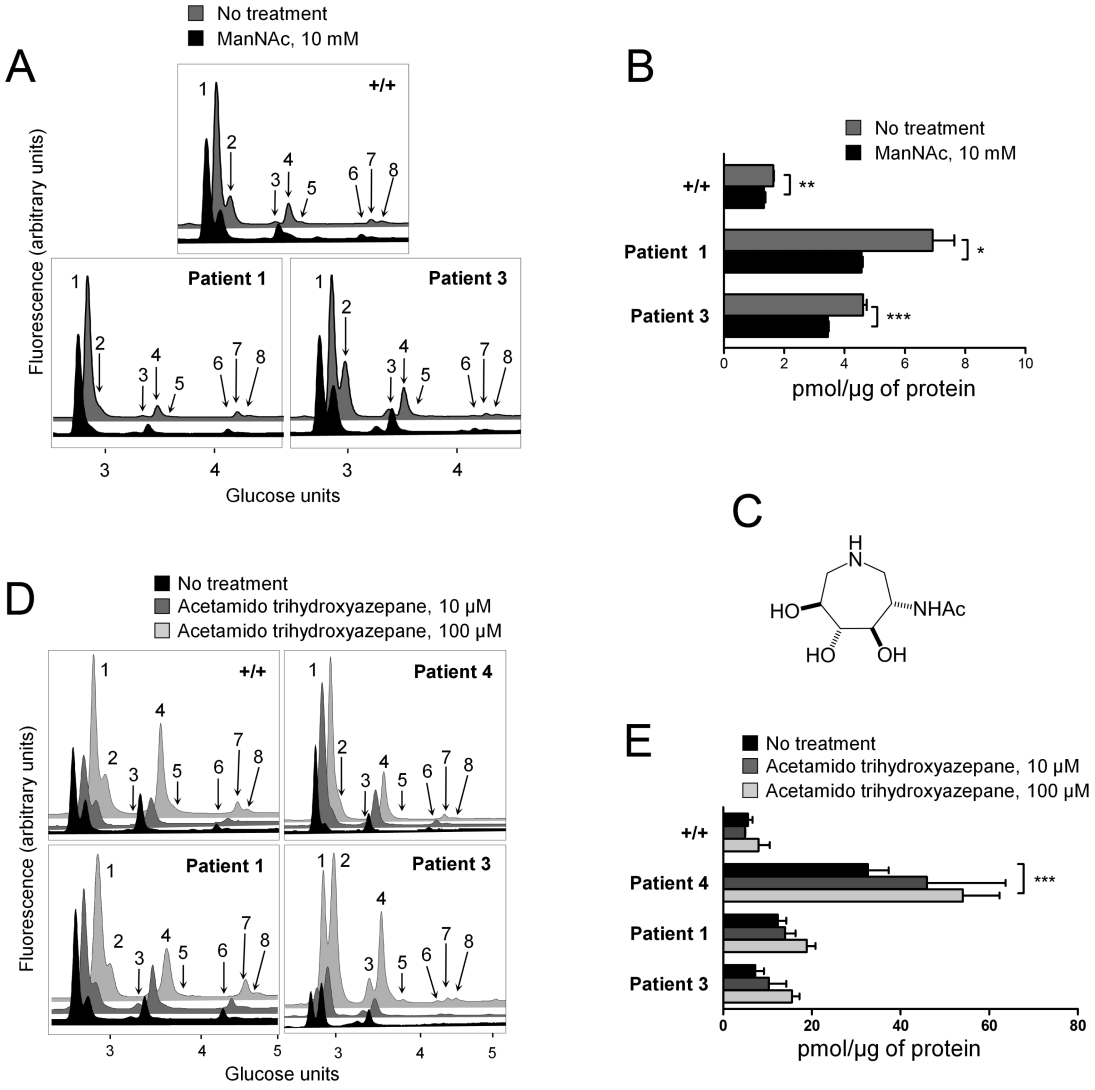

Fig. 2. Manipulation of the sialic acid synthesis pathway alters GSL concentrations.

A: HPLC analysis of 2-AA labeled GSL-derived glycans from fibroblasts grown in 2% FCS media with (black) or without (grey) 10 mM ManNAc. Peak numbers refer to structures in Fig. 1A. Chromatograms are adjusted for total protein.

B: Total GSL levels in cells treated as in A.

C: Chemical structure of acetamido trihydroxyazepane [22].

D: HPLC analysis of 2-AA labeled GSL-derived glycans purified from fibroblasts grown for one week in 10% FCS and two weeks in 2% FCS in the absence (black) or presence of acetamido trihydroxyazepane [22] at 10 μM (dark grey) or 100 μ M (light grey). Chromatograms are adjusted for total protein.

E: Total GSL concentrations in cells treated as in D. Results in bar graphs represent mean ± SEM (n=3) *P<0.05, **P<0.01, ***P<0.001 (two tailed unpaired Student's t-test).

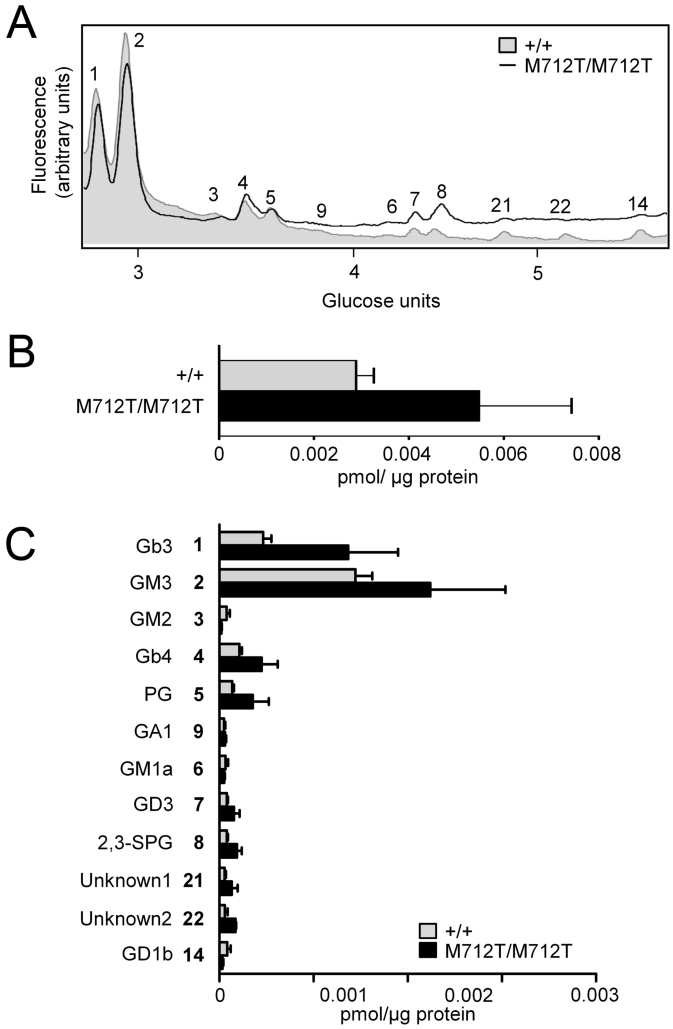

Fig. 3. Total GSL concentration is elevated in GNE myopathy patients' plasma.

A: HPLC analysis of 2-AA labeled GSL-derived oligosaccharides purified from control (n=3) and GNE myopathy patients' plasma (n=2; both harboring a homozygous p.M712T mutation in GNE). Peak numbers correspond to structures in Fig. 1A. Chromatograms are adjusted for total protein.

B: Total GSL concentrations from control and patients' plasma.

C: Plasma concentrations of individual GSL species, as outlined in **A**.

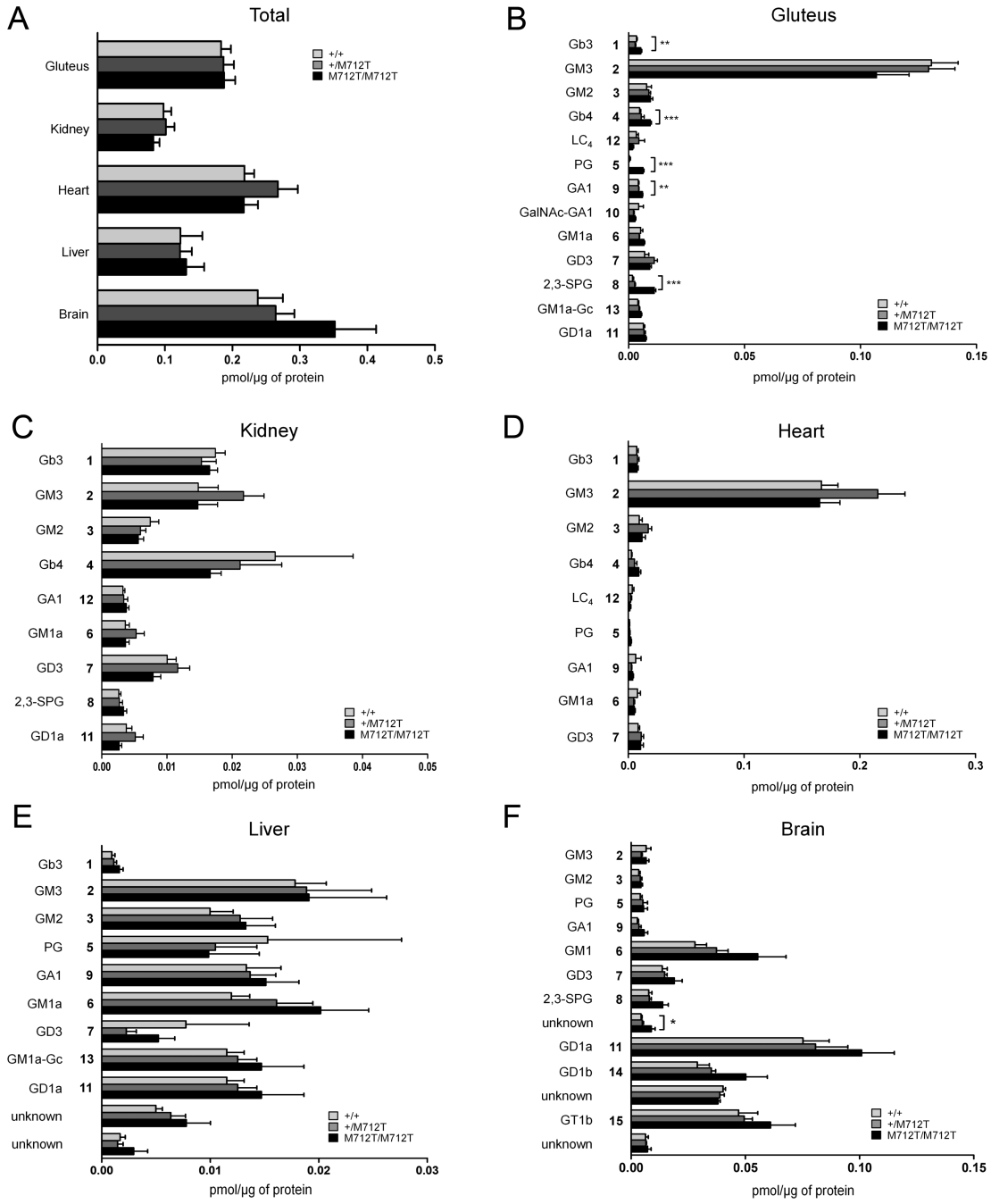

Fig. 4. Sialylated and neutral GSLs are dysregulated in *Gne*$^{M712T/M712T}$ mouse tissue

HPLC analysis of 2-AA-labeled ceramide glycanase-released oligosaccharides from GSLs purified from P2 tissues of a GNE myopathy knock-in mouse model. Levels of GSLs are expressed in pmol per 1 μg total protein. GSL numbers refer to structures in Fig. 1A. Each bar represents mean ± SEM (n≥5) *P<0.05, **P<0.01, ***P<0.001 (two-tailed unpaired Student's t-test). **A,** Total GSL, **B** Gluteus (skeletal muscle), **C**, Kidney, **D**, Heart, **E**, Liver, **F**, Brain.